

SCALE INVARIANT PROPERTIES IN HEART RATE SIGNALS*

DANUTA MAKOWIEC, ALEKSANDRA DUDKOWSKA, MARCIN ZWIERZ

Institute of Theoretical Physics and Astrophysics, Gdańsk University
Wita Stwosza 57, 80-952 Gdańsk, Poland

RAFAŁ GAŁAŚKA, ANDRZEJ RYNKIEWICZ

1st Department of Cardiology, Medical University of Gdańsk
Dębniaki 7, 80-211 Gdańsk, Poland

(Received March 1, 2006)

The rate of heart beat is controlled by autonomic nervous system: accelerated by the sympathetic system and slowed by the parasympathetic system. Scaling properties in heart rate are usually related to the intrinsic dynamics of this physiological regulatory system. The two packages calculating local exponent spectra: Wavelet Transform Modulus Maxima and Multifractal Detrended Fluctuation Analysis (accessible from Physionet home page <http://circ.ahajournals.org/cgi/content/full/101/23/e215>) are tested, and then used to investigate the spectrum of singularity exponents in series of heart rates obtained from patients suffering from reduced left ventricle systolic function. It occurs that this state of a heart could be connected to some perturbation in the regulatory system, because the heart rate appears to be less controlled than in a healthy human heart. The multifractality in the heart rate signal is weakened: the spectrum is narrower and moved to higher values what indicate the higher activity of the sympathetic nervous system.

PACS numbers: 87.19.Hh, 05.40.-a, 87.80.Vt, 89.75.Da

1. Introduction

Heart rate variability (HRV) represents one of the most promising marker for measuring activity of the autonomic nervous system — the system that is responsible for cardiovascular mortality [1]. The wide popularity of HRV

* Presented at the XVIII Marian Smoluchowski Symposium on Statistical Physics, Zakopane, Poland, September 3–6, 2005.

study is ensured by the noninvasive, easily obtainable techniques providing a signal to analysis [1–4]. The electrocardiogram (ECG), a recording of cardiac-induced potential, reveals the basic information about atrial and ventricular electrical activity of the heart. Readily recognizable features of ECG are labeled by the letters P–QRS–T, see Fig. 1. In a continuous ECG record each QRS complex is detected, and the so-called normal-to-normal (NN) intervals are determined. Hence, the ECG signal is simplified to moments of contractions only. These moments are identified by R peaks.

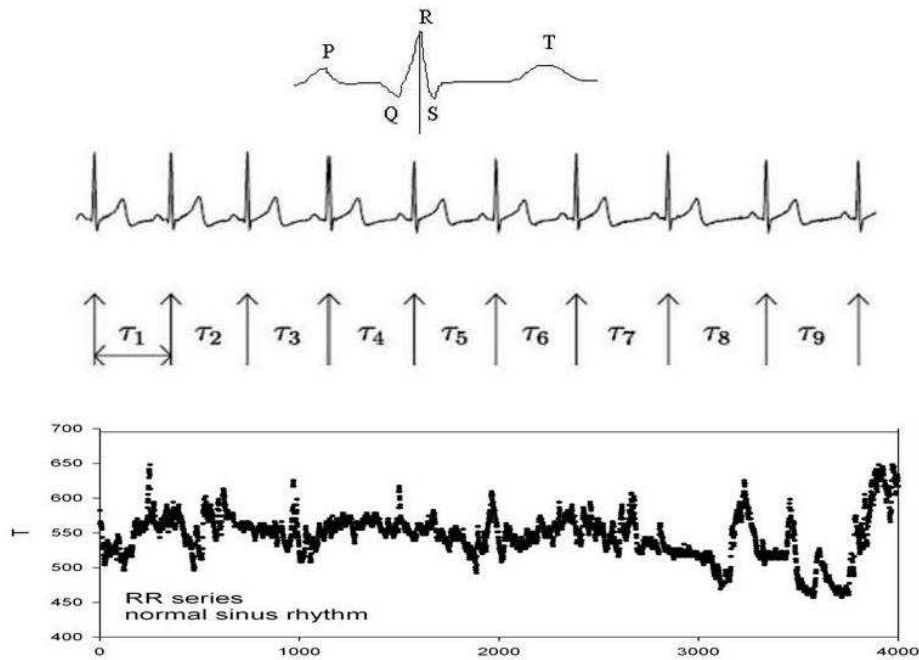


Fig. 1. From the top: an ECG record of a single heart beat with labels of P,Q,R,S, and T, a representative record of ECG signal for a healthy subject, RR-signal $\{\tau_i\}$ extracted from subsequent R peaks, a representative RR-signal for normal sinus rhythm of 4000 beats (approximately 1 hour).

In mathematical terms, the heartbeat signal is modeled as a point process. The occurrence of a contraction at time t_i is represented by an impulse of Dirac delta function $\delta(t - t_i)$, so that the sequence of heartbeats is as follows

$$X(i) = \sum_i \delta(t - t_i). \quad (1)$$

Any realization of a point process is specified by the set of occurrence times $\{t_i\}$ of these events. The RR-signal $\{\tau_i\}$ is a sequence of positive numbers representing adjacent times $\tau_i = t_{i+1} - t_i$. Hence, the widely studied RR-signal is the series of intervals between the consecutive normal R peaks.

The ectopic beats or arrhythmic events which are present in the ECG record and which are not represented in RR series are beside the scope of our investigations, though we remember about their role in quantifying the heart state, see *e.g.* [5] for further information.

Scale invariance of a time series means that no specific scale of time can be identified in the data under study. It implies that the common data analysis procedures based on searching for the characteristic scale have to be replaced by new ones. These procedures, aiming on analysis of relationship between scales, provide an insight on mechanisms that relate scales.

Physiologic signals are known to have scale invariant properties. A heart rate of a healthy human shows long-range temporal correlations [6, 7], non-Gaussianity of the probability density function of $\{\tau_i\}$ [6] and multifractal scaling properties [8, 9]. These properties are conjectured to be related with interactions among many individual components driven by competing forces operating near the critical point of their phase space [10, 11]. The rate of heart beat is controlled by autonomic nervous system: accelerated by the sympathetic system and slowed by the parasympathetic system. Multifractal scaling in heart rate requires the existence of the balance between antagonistic activity of parasympathetic and sympathetic system. For example, congestive heart failure is known to be associated with both increased sympathetic system activity and decreased parasympathetic system activity. The multifractal properties of a RR-signal are reduced to monofractal ones. Moreover, if parasympathetic blocker — atropine, is served to a healthy subject then a collapse of the multifractal spectrum is observed while heart-beat dynamics during sympathetic blockade display a small change in the multifractal spectrum [12]. Furthermore, the conservation of multifractal properties is observed in RR-series of patients with clinically recognized autonomic system dysfunction (loss of sympathetic neurons) [13]. Therefore the origin of heart rate complexity is searched in the intrinsic dynamics of this physiological regulatory system. Although the exact mechanism of the heart beat is unknown [14] some attempts are done [15].

The question posed by us here is whether the heart disease called reduced left ventricular systolic function is associated with the failure of the autonomic antagonistic activity between parasympathetic and sympathetic nervous systems. It is known that early left ventricular dysfunction elicits the changes in the autonomic nervous system: activates of sympathetic drive and attenuates of parasympathetic tone in case of recognised congestive heart failure [16]. The widely used NYHA classification [1] evaluates an

efficient heart as the I class, and with increasing class number the efficiency of a heart is smaller. The IV class denotes a heart almost not working. The patients considered by us are classified within the NYHA I–III classes while the congestive heart failure gives NYHA III,IV classes. Therefore, the change in the fractal properties is not obvious.

In the next section we introduce the multifractal method of data analysis and show results of tests of the methods applied to series with known properties. Section 3 contains the main results of analysis on the data prepared in the 1st Department of Cardiology of Medical University of Gdańsk. These data can be obtained on request [32]. Our investigations suggest that reduced left ventricular systolic function of a heart could be related to some perturbation in the regulatory system. The heart rate appears to be less controlled than in a case of a healthy human heart. The multifractality in the heart rate signal is weakened: the spectrum is narrower and moved to higher values.

2. Numerical procedures and tests

2.1. Multifractal formalism

Multifractal formalism is the way to study scale invariance of time series in their whole variety and dependences [19,20]. The easily recognizable sign of the scale invariance of a $X(t)$ process is the occurrence of scaling in any of its statistics, called a structure function.

For example, let us consider as the structure function the statistics of q -moments of increments of a process $X(t)$ in a scale δ , namely:

$$\langle |X(t + \delta) - X(t)|^q \rangle \propto |\delta|^{\tau(q)}. \quad (2)$$

Then a relevant analysis of scaling phenomena means estimates of the corresponding scaling exponents $\tau(q)$ (called a partition function). A stochastic processes exhibiting scaling in their statistics is called a fractal stochastic process.

Depending on relation of τ on q , a process is called:

- *monofractal* — if a partition function is linear,
- *multifractal* — any other dependence.

The q -dependence of a partition function is mapped into ubiquitous occurrences of irregularities, called local singularities spectrum or multifractal spectrum: the set of pairs: $\{(h, D(h))\}$ where h is the local singularity exponent and $D(h)$ is the fractal dimension of the subset of the original time series characterized by the local scaling exponent h , by the Legendre transform:

$$h = \frac{d\tau(q)}{dq}, \quad D(h) = qh - \tau(q). \quad (3)$$

The most prominent example is the fractional Brownian motion $B_H(t)$ [22] labeled by H the Hurst exponent. Since at any scale δ the following self-similarity relation holds:

$$B_H(\delta t) \equiv_{\text{prob}} \delta^H B_H(t) \quad (4)$$

then all local $h(t)$ exponents are not dependent on t , and $h(t) = H$.

There exists a mathematically rigorous approach to fractional Brownian motions [20–22] and to their generalizations, to the, so-called random cascades and process of the compound Poisson cascade [23] which explains fractality by multiplicative organization of a signal. Multiplicative cascades are built from iterative split/multiply procedures that hence produce interdependencies between the different scales of the resulting process.

In case of continuous real signals arising from *e.g.* fully developed turbulence [24, 25], or financial time series [19, 26], or load of network traffic [27], multiplicative signal organization can be directly related. The singularity spectrum is accessible by, for example, the wavelet analysis [28]. However, a sequence of events extracted from human heart electrocardiogram is different from signals originally studied by multifractal formalism. Instead of the singularity spectrum, the multifractal formalism provides a spectrum of, so-called, local Hurst exponents [8–11].

2.2. Numerical procedures

A numerical computation straight from the definition is obviously not feasible. The local singularity exponents vary widely from point to point making their numerical measurement extremely unstable. The way out consists in obtaining the desired multifractal spectrum via carefully designed structure function. The following two methods to construct the structure function have been proposed

WTMM — Wavelet Transform Modulus Maxima [28]

Here the multiresolution analysis of a signal is done by the wavelet theory. A partition function $\tau(q)$ is found from a power-law dependence $Z(q, \delta) \propto \delta^{\tau(q)}$ where the structure function $Z(q, \delta)$ is the sum of the q th powers of the local maxima of the absolute moduli of the wavelet transform coefficients at scale δ . In this study the third derivative of the Gaussian function is used as the analysing wavelet.

MDFA — Multifractal Detrended Fluctuation Analysis [29]

Here the multiresolution analysis bases on DFA method [17]. The integrated signal is divided into scales of δ size. In each j -th box the variance of the integrated and detrended signal is calculated $F^2(\delta, j)$.

The partition function $\tau(q)$ is found from the structure function $F(q, \delta)$ constructed as the mean of the $q/2$ -th powers of $F^2(\delta, j)$ over all boxes of δ length $F(q, \delta) \propto \delta^{1+\tau(q)}$.

We use the software accessible from Physionet [31] to calculate partition functions. Namely, we work with two packages: DFA.C (prepared by J. Mietus, C.-K. Peng, and G. Moody) and MULTIFRACTAL.C (prepared by Y. Ashkenazy). We perform the following tests to investigate the packages abilities:

1. White noise and random walk signals

Series are generated by `rand48()` function. The expected result is a partition function $\tau(q)$ linearly dependent on q with coefficient 0 for white noise and 0.5 for a random walk. The results are shown in Fig. 2. One should notice large departures from the theoretical predictions. The MDFA method correctly finds the spectrum of white noise — the point spectrum located at $(0,1)$.

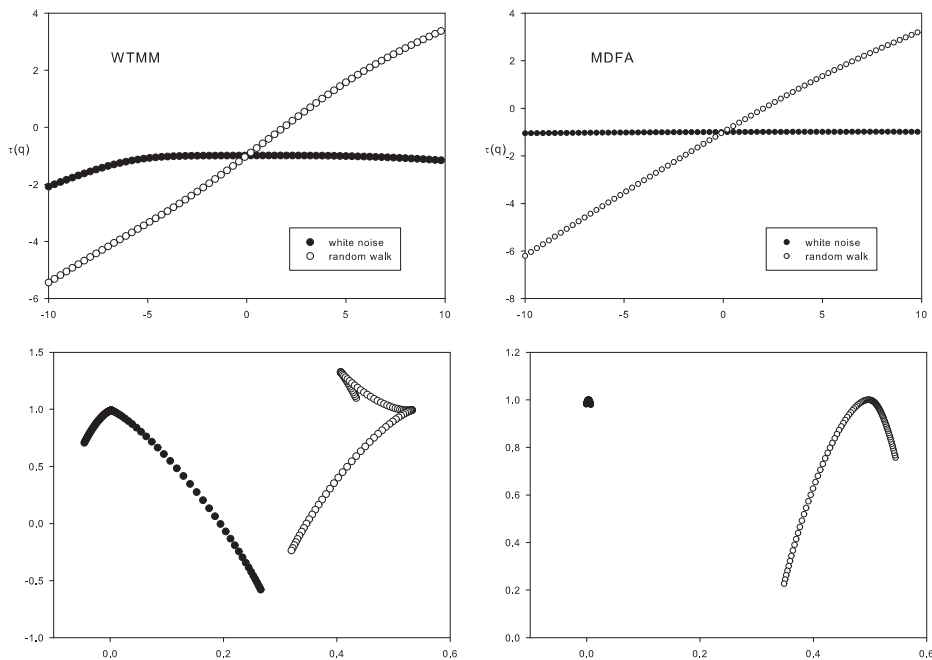


Fig. 2. Partition functions $\tau(q)$ for $q \in [-10, 10]$ (top) and resulting multifractal spectrum (bottom) for white noise and random walk signals. The series length is 20000. The multivalued picture of the WTMM spectrum of random walk is related to (3), *i.e.*, to sensitivity of numerical differentiation to any departure from a line.

2. Fractional noises

Series are generated with the help of tsfBm-package [30]. The results are shown in Fig. 3. It is easy to notice that the partition functions are not linearly dependent on q in all cases and especially in case of WTMM method when high negative q is investigated. It results that the corresponding spectrum is not point-like as it is expected but has a large width. This width is related with the method. Basically, a wider spectrum is obtained for WTMM method. However, the maximum of the spectrum lines is close to the theoretical values $(H,1)$ in both methods.

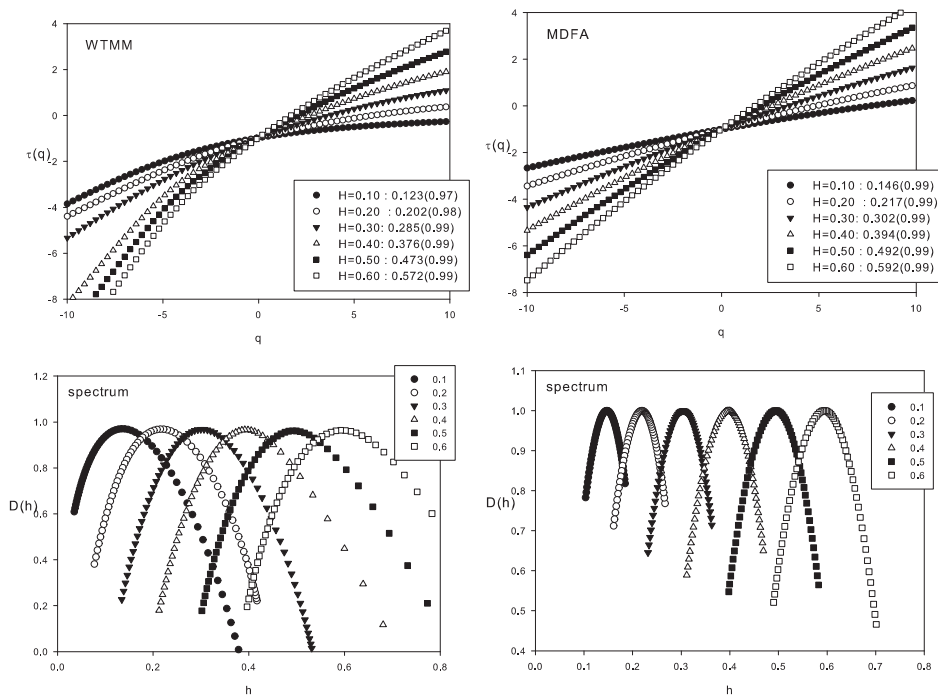


Fig. 3. Partition functions $\tau(q)$ for $q \in [-10, 10]$ (top) and resulting multifractal spectrum (bottom) for monofractal signals with Hurst exponent shown by labels. The linear fit coefficients estimated by r^2 Pearson correlation coefficient are shown at labels. The series length is 20000.

The multifractal properties in heart rate signals have been discovered in the data collected on Physionet page [31]. To calibrate better our numerical tools we perform the multifractal analysis on the Physionet data too. To observe the multi- to mono-fractal transition, we consider 24-hour series

of 14 healthy subjects: **nsr**-group and 12 subjects with congestive heart failure: **chf**-group. For each series the 5-hour long subseries are extracted corresponding to diurnal (wake) human activity. Fig. 4 collects results of the analysis.

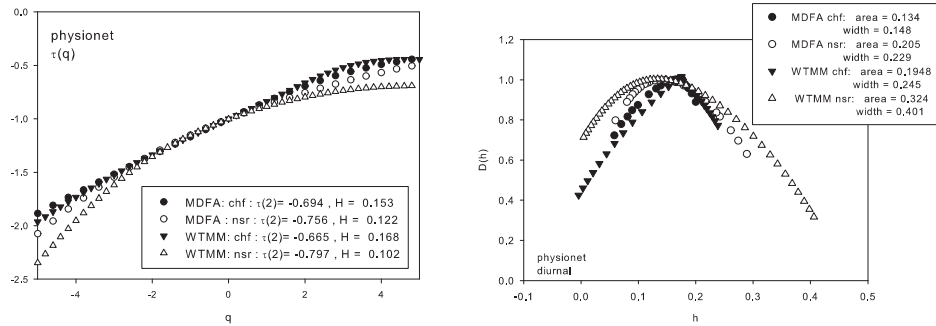


Fig. 4. Left: mean partition functions $\tau(q)$ for $q \in [-5, 5]$ for heart rate signals from Physionet: normal sinus rhythm (nsr) mean group and congestive heart failure (chf) mean group. At curve labels the global Hurst exponents are shown. Right: the spectra of nsr group and chf group. At curve labels the multifractal characteristics are added: the width and area below the curve.

The spectra obtained by both methods display the expected properties: the shrinkage of the h interval when one moves from healthy to failure hearts and the change in the shape of spectra from a parabola-wide to triangle-like shape. Both properties ensure that variety of the scaling exponents vanishes in case of congestive heart failure.

Since the multifractal formalism gives the direct estimate for the global Hurst exponent: $H = \frac{1}{2}(1 + \tau(2))$, let us notice that the global Hurst exponents calculated from our analysis restore the known relation: $H(\text{nsr}) < H(\text{chf})$ which is interpreted as less control in case of chf. Moreover, by both methods the basic properties quantifying the multifractal spectra properties such as width of the spectra curve and the area below the spectra curve provide significantly larger values for healthy heart series than values obtained for hearts with congestive heart failure.

3. Multifractal properties related to reduced left ventricular systolic function

The multifractal properties are estimated for RR-series collected and selected from patients treated in Medical University of Gdańsk [32]. The 24h ECC Holter monitoring was performed in the group of 40 subjects with normal echocardiogram, without past history of cardiovascular diseases:

gk-group, and in the group of 90 patients with reduced left ventricular systolic: **nk**-group. ECG data were recorded and digitized using Delmar Avionics recorder. Recordings were analyzed and annotated using Delmar Accuplus 363 system by an experienced physician. The two 5 hours subsets were extracted from each obtained data set corresponding to different stages of human activity: nocturnal (sleep) and diurnal (wake).

For each series the partition function $\tau(q)$ is calculated by both methods: WTMM and MDFA for $q = -5, \dots, 5$ with a $dq = 0.1$ step. Then the group averaged partition function is found. These results together with their standard deviation errors to underline variability of the results are presented in Fig. 5. In case of MDFA method the errors are significantly smaller.

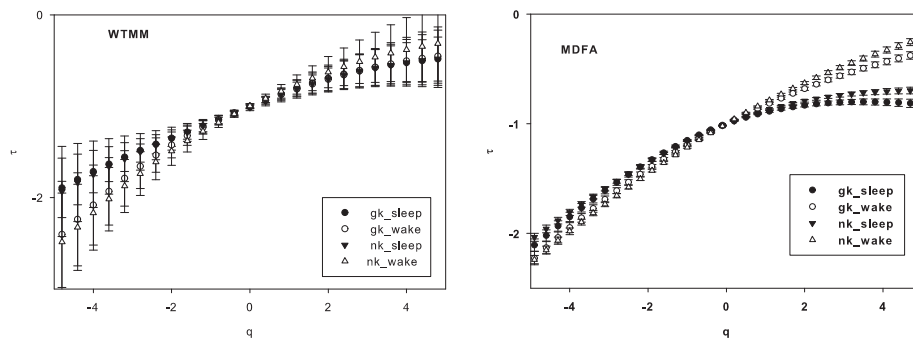


Fig. 5. Mean partition functions $\tau(q)$ for $q \in [-5, 5]$ representing the group means obtained by different methods (for better figure readability only every third point is plotted, the standard deviation errors are added).

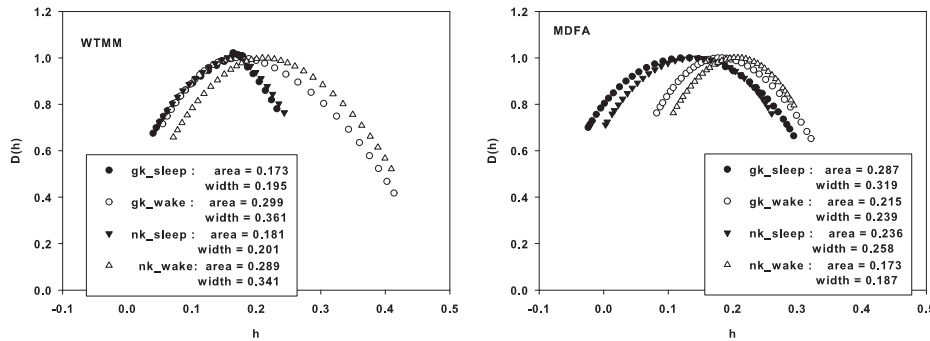


Fig. 6. Multifractal spectra of gk_{wake} , gk_{sleep} , nk_{wake} and nk_{sleep} groups obtained by different methods. At curve labels the multifractal characteristics are added: the width and area below the curve.

Both methods find the difference between spectra, see Fig. 6 when the wake parts of series are considered. The spectra widths and spectra areas in case of gk-group are larger then in nk-group, however the difference is not as significant as in case of congestive heart failure. This indicates at the loss of multifractality but the loss is weaker than the change to monofractal case. Moreover, the localizations of the spectra are changed — they are moved to higher h values — more anticorrelations are present in the signal. This can be interpreted as an indication that the heart with reduced left ventricle systolic is less controlled than the healthy heart. Surprisingly, the stronger control mechanisms can be found in the sleep series — the spectra are moved to lower h values. However, the nocturnal series do not provide a clear answer about the multifractality — WTMM method indicates a significant loss of fractality while MDFA suggests even an increase in fractality. This result can be related with algorithms leading to a partition function. For

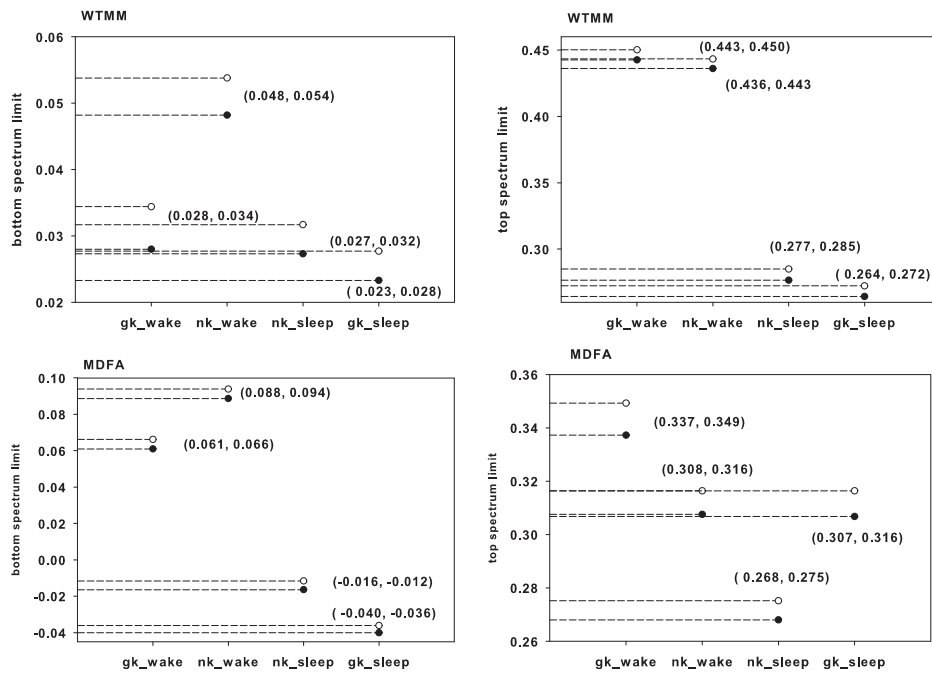


Fig. 7. The minimal (left) and maximal (right) 95-confidence intervals of h -value in case the multifractal study is for $q \in [-5, 5]$.

the diagnostic purpose it could be useful to clarify the differences between groups by determining limits of the corresponding group spectra. In Fig. 7 we present the group averages of the localization of the spectra by plotting the minimal (bottom) and maximal(top) values of spectra together with

95-confidence error intervals. It appears that with the help of MDFA method a healthy heart can be successfully discriminated from a heart with reduced left ventricular systolic function.

4. Closing

In the paper we investigated if the reduced left ventricular systolic function could be associated to the imbalance in the control mechanism of autonomous nervous system. It is known that this imbalance affects the multifractal spectra of a heart rate signal by decreasing the multifractality.

The study was done by two methods- WTMM and MDFA. Both methods used software packages easily accessible from Internet. These methods were carefully tested to find out best parameters for the multifractal analysis of heart rate signals.

By both methods the loss of multifractality was observed though this loss could not be recognized as a change to monofractal case. Moreover, since the localizations of the spectra were changed, we could conclude that the heart with reduced left ventricle systolic was less controlled than the healthy heart. However, we found the strong control mechanisms in the sleep series.

Moreover, due to the low errors MDFA method could be practically used to discriminate a healthy heart from a heart with reduced left ventricular systolic function.

Summing up, the multifractal analysis performed by us indicated that in the disease of reduced left ventricular systolic function the imbalance in the autonomic nervous system relies on activation of sympathetic nervous system rather and only weak deactivation of parasympathetic nervous system is noticed.

We wish to acknowledge the support of the Rector of Gdańsk University — project: BW/5400-5-0166-5.

REFERENCES

- [1] Heart Rate Variability. Standards of Measurement, Physiological Interpretation, and Clinical Use. Task Force of The European Society of Cardiology and The North American Society of Pacing and Electrophysiology, *European Heart Journal* **17**, 354 (1996).
- [2] A.L. Goldberger, Nonlinear Dynamics, Fractals, and Chaos Theory: Implications for Neuroautonomic Heart Rate Control in Health and Disease, in *The Autonomic Nervous System* eds. C.L. Bolis, J. Licinio, World Health Organization, Geneva 1999.
- [3] L. Glass, P. Hunter *Physica D* **43**, 1 (1990).

- [4] M.C. Teich, S.B. Lowen, B.M. Jost, K. Vibe-Rheymer, C. Heneghan. Heart Rate Variability: Measures and Models, pp. 159-213 in *Nonlinear Biomedical Signal Processing. Vol. II. Dynamic Analysis and Modeling* ed. M. Akay, IEEE Press, New York 2001.
- [5] H.-X. Wang, R. De Paola, W.I. Norwood, *Phys. Rev. Lett.* **70**, 3671 (1993); **71**, 3039 (1993); K. Takayanagi, K. Tanaka, H. Kamishirado, Y. Sakai, T. Fujito, I. Inoue, T. Hayashi, S. Morooka, N. Ikeda, *J. Cardiovasc. Electrophysiol.* **11**, 168 (2000); L.S. Liebovitch, A.T. Todorov, M. Zochowski, D. Scheuerle, L. Colgin, M.A. Woods, K.A. Ellenbogen, J.K. Heere, R.C. Bernstein, *Phys. Rev.* **E59**, 3312 (1999); V. Sculte-Frhlinde, Y. Ashkenazy, A.L. Goldberger, P.Ch. Ivanov, M. Costa, A. Morley-Davis, H.E. Stanley, L. Glass, *Phys. Rev.* **E66**, 031901 (2002).
- [6] C.-K. Peng, J. Mietus, J.M. Hausdorff, S. Havlin, H.E. Stanley, A.L. Goldberger, *Phys. Rev. Lett.* **70**, 1343 (1993).
- [7] Y. Yamamoto, R.L. Hughson, *Am. J. Physiol.* **266**, R40 (1994).
- [8] P.Ch. Ivanov, M.G. Rosenblum, C.-K. Peng, J. Mietus, S. Havlin, H.E. Stanley, A.L. Goldberger, *Nature* **383**, 323 (1999).
- [9] P.Ch. Ivanov, M.G. Rosenblum, C.-K. Peng, J.E. Mietus, S. Havlin, H.E. Stanley, A.L. Goldberger, *Physica A* **249**, 587 (1998); H.E. Stanley, L.A.N. Amaral, A.L. Goldberger, S. Havlin, P.Ch. Ivanov, C.-K. Peng, *Physica A* **270**, 309 (1999); S. Havlin, L.A.N. Amaral, Y. Ashkenazy, A.L. Goldberger, P.Ch. Ivanov, C.-K. Peng, H.E. Stanley, *Physica A* **274**, 99 (1999).
- [10] P.Ch. Ivanov, L.A.N. Amaral, A.L. Goldberger, S. Havlin, M.G. Rosenblum, H.E. Stanley, Z.R. Struzik, *Chaos* **11**, 641 (2001).
- [11] P.Ch. Ivanov, Z. Chen, K. Hu, H.E. Stanley, *Physica A* **344**, 685 (2004).
- [12] L.A.N. Amaral, P.Ch. Ivanov, N. Aoyagi, I. Hidaka, S. Tomono, A.L. Goldberger, H.E. Stanley, Y. Yamamoto, *Phys. Rev. Lett.* **86**, 6026 (2001).
- [13] Z.R. Struzik, J. Hayano, S. Sakata, S. Kwak, Y. Yamamoto, arXiv:q-bio.0T/0410001.
- [14] K. Kiyono, Z.R. Struzik, N. Aoyagi, S. Sakata, J. Hayano, Y. Yamamoto, *Phys. Rev. Lett.* **93**, 178103 (2004).
- [15] K. Kotani, Z.R. Struzik, K. Takamasu, H.E. Stanley, Y. Yamamoto, *Phys. Rev.* **E72**, 041904 (2005).
- [16] G.M. Eaton, R.J. Cody, E. Nunziata and P.F. Binkley, *Circulation* **95** 555
- [17] C.-K. Peng, S. Havlin, H.E. Stanley, A.L. Goldberger, *Chaos* **5**, 82 (1995).
- [18] P.Ch. Ivanov, J.M. Hausdorff, S. Havlin, L.A.N. Amaral, K. Arai, V. Schulte-Frohlinde, M. Yoneyama, H.E. Stanley, con-mat/0409545.
- [19] B.B. Mandelbrot *The Fractal Geometry of Nature*, W.H. Freeman, 2nd ed., New York 1983.
- [20] K.J. Falconer, *Fractal Geometry — Mathematical Foundations and Applications*, Second Edition, John Wiley, 2003.
- [21] R.H. Riedi, in *Long-Range Dependence: Theory and Applications*, eds. P. Doukhan, G. Oppenheim, M.S. Taqqu, Cambridge Ma, Birkhäuser 2001, pp. 625–716

- [22] E. Bacry, J. Delour, J.F. Muzy, *Phys. Rev.* **E64**, 026103 (2001).
- [23] J. Barral, B. Mandelbrot, *Prob. Theory and Related Fields* **124**, 409 (2002).
- [24] B.B. Mandelbrot, *J. Fluid Mech.* **62**, 331 (1974); R. Benzi, G. Paladin, G. Parisi, A. Vulpiani, *J. Phys. A* **17**, 3521 (1984).
- [25] U. Frisch, G. Parisi, Proc. Int. Summer School on Turbulence and Predictability in Geophysical Fluid Dynamics and Climate Dynamics, 1985, pp. 84–88.
- [26] B. Mandelbrot, *Fractals and Scaling in Finance*, Springer, New York 1997; J.F. Muzy, D. Sornette, J. Delour, A. Arnedo, *Quantitative Finance* **1**, 131 (2001).
- [27] R. Riedi, J. Lévy Véhel, Technical Report No 3129, INRIA Rocquencourt, France, Feb 1997, see also J. Lévy Véhel, R. Riedi, *Fractals in Engineering*, Springer 1997, pp. 185–202.
- [28] E. Bacry, J.F. Muzy, A. Arnedo, *J. Stat. Phys.* **70**, 635 (1993); J.F. Muzy, E. Bacry, A. Arnedo, *Phys. Rev.* **E47**, 875 (1993).
- [29] J.W. Kantelhardt, S.A. Zschiegner, E. Koscielny-Bunde, S. Havlin, A. Bunde, H.E. Stanley, *Physica A* **316**, 87 (2002).
- [30] J. Conover, <http://www.johncon.com/> Copyright © 1994-2005, John Conover, All Rights Reserved.
- [31] A.L. Goldberger, L.A.N. Amaral, L. Glass, J.M. Hausdorff, P.Ch. Ivanov, R.G. Mark, J.E. Mietus, G.B. Moody, C.K. Peng, H.E. Stanley, PhysioBank, PhysioToolkit, and PhysioNet: Components of a New Research Resource for Complex Physiologic Signals. *Circulation* 101(23):e215-e220 [Circulation Electronic Pages; <http://circ.ahajournals.org/cgi/content/full/101/23/e215>]; 2000 (June 13).
- [32] All series considered by us can be obtained on request ola@iftia9.univ.gda.pl